A Precuneal Causal Loop Mediates External and Internal Information Integration in the Human Brain

Dian Lyu[1,2], Ioannis Pappas[1,3], David K. Menon[1,4], Emmanuel A. Stamatakis[1,2,*]

[1]University Division of Anaesthesia, University of Cambridge,

Addenbrooke's Hospital, Hills Rd, CB2 0SP Cambridge, U.K.

[2]Department of Clinical Neuroscience, University of Cambridge,

Addenbrooke's Hospital, Hills Rd, CB2 0SP Cambridge, U.K.

[3]Helen Wills Neuroscience Institute, University of California, Berkeley, CA, 94720, U.S.A.

[4]Wolfson Brain Imaging Centre, University of Cambridge,

Cambridge Biomedical Campus (Box 65), CB2, 0QQ, Cambridge, U.K.

[*]To whom correspondence should be addressed; E-mail: eas46@cam.ac.uk

Supplementary Materials

Experiment descriptions for the task-related fMRI data

The N-back Working Memory (N-back) task We adopted two visual-based and attention-demanding tasks from the available tasks in HCP. One of them is the N-back task which was designed to test working memory capacity. To maximise efficiency, visual stimuli (i.e. images of common objects) were divided into 4 specific categories (faces, places, tools and body parts), one category per block. In the present project we ignored object types but only focused on the effect of cognitive effort by contrasting between the "0-back" and the "2-back" conditions.

In both conditions, participants were presented with a series of objects, one at a time. The 2-back condition requires more memory load than the 0-back condition, as participants in this situation must respond (i.e. press a button) as soon as they see an object that is the same as the one presented two objects before. Whereas in the 0-back condition, a target object was presented at the start of each block, and participants only respond to the "target" regardless of the presented sequence.

The experiment contained 8 task blocks (each having 10 trials, 2.5 s per trial or 25 s per block) and 4 fixation blocks (15 s per block); half of the task blocks were for the 2-back condition and another half for the 0-back condition. On each trial, the stimulus was presented for 2 s, followed by a 500ms inter-trial interval (ITI). At the start of the block, a 2.5-s cue was presented to inform participants of the condition type.

The higher-order relational processing (RP) task The other task we chose from the HCP was the higher-order relational processing task. This task tests the ability for understanding hidden relationships between objects, which is the basis of concept formation and logical reasoning.

The experiment contains 6 task blocks divided by three 16 (s) fixation blocks, in an order of every two task blocks being followed by a fixation block. Among the concatenated task blocks, one is the more difficult "relational processing" condition, which contained 4 trials with 3500 ms stimuli presentation and 500 ms ITI per trial; and the other is the easier "matching" condition, containing 5 trials with 2800 ms stimuli presentation and 400 ms ITI per trial. The visual stimuli were 6 geometric shapes filled with 6 alternative textures, which were generated by a randomised process. For the relational processing condition, the stimuli were presented for 3500 ms, with a 500 ms ITI, with four trials per block. In the matching condition, stimuli were presented for 2800 ms, with a 400 ms ITI, with 5 trials per block. Each type of block (relational or matching) lasted a total of 18

s. In the relational processing condition, participants were presented with 2 pairs of objects aligned in two rows, one at the top and one at the bottom of the screen. The participants were asked to determine whether the 2 objects of one pair (at the same row) are different in the same way (e.g. either in shape or texture) as the other pair below. Whereas in the match condition, the participants were shown 3 objects, one pair at the top and a single one at the bottom, and the participants only needed to determine whether the bottom object matched either one of the two objects on top in a specified feature, such as in shape when the word "shape" is prompted in the middle of the screen. The relational processing condition tests the ability of inferring an inner relationship (a common feature) between two pairs of different objects, apart from recognising different features embedded in an object like in the match condition.

Resting-state (rs)FC of the dPCu and vPCu

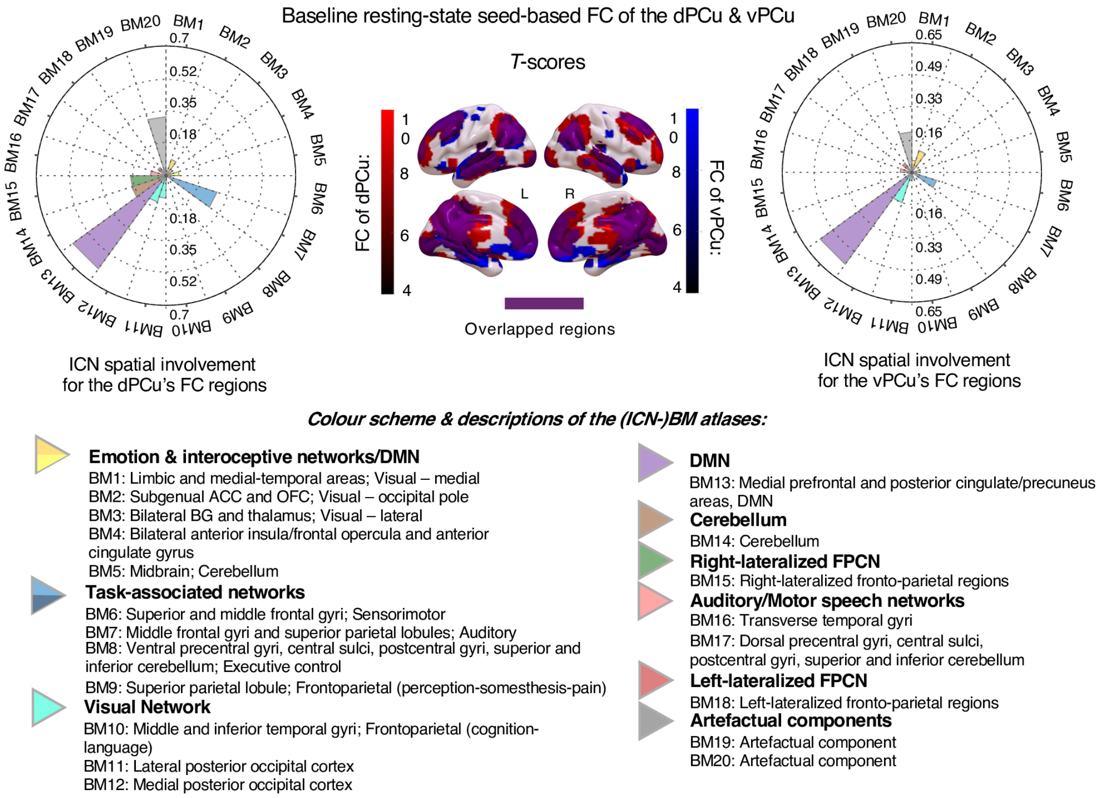

Figure S1. Resting-state seed-based FC of the d/vPCU. The middle panel shows the dPCu is functionally connected with the red regions and the vPCu is functionally connected with the blue regions in the brain. Purple indicates overlap between the d/vPCu's FC. The circular wedge plots on the left and right indicate the ICN spatial involvement for the significant brain regions having the resting-state FC of the d/vPCu. The spatial localisation of the ICNs is provided by the BrainMap/BM-ICN atlases from the *ICN_atlas* toolbox. Cognitive domains and descriptions of the BM/ICN atlases for the ICNs are also provided below. The same colour scheme was used throughout the paper.

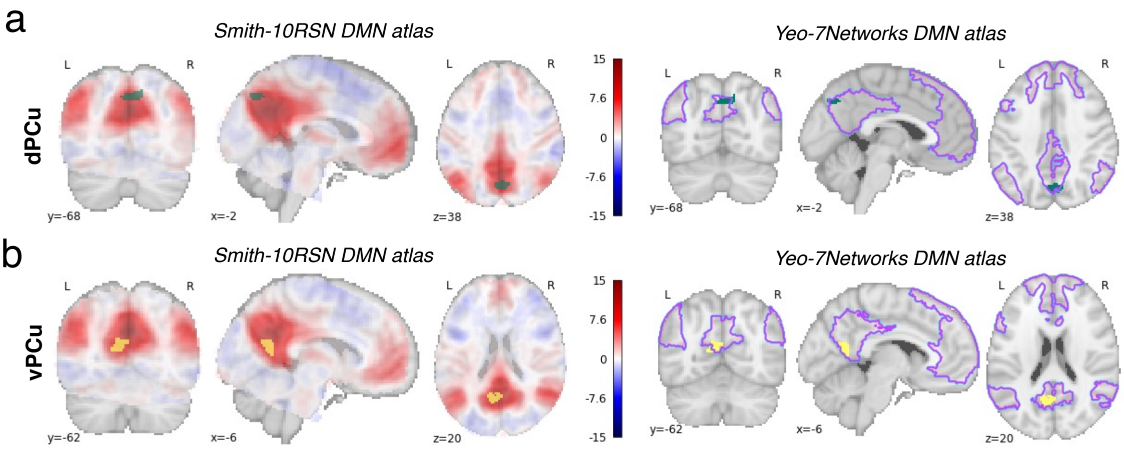

Figure S2. Spatial localisation of the dPCu (a) and vPCu (b) respective to the canonical DMN. For the probabilistic *Smith-10RSN* atlas, the brain heatmap is the z-score map for the ICA component that corresponds to the canonical DMN. For the deterministic *Yeo-7Networks* atlas, the edges of the DMN are outlined with purple lines. The seeds are superimposed upon the DMN atlases, with the dPCu colored with green and vPCu colored with Yellow.

Correspondence of brain regions to ICNs between atlases

We used two types of atlases for labelling our significant clusters to provide readers a more unbiased evaluation of the anatomical correspondence of our results. One is the functionally-defined brain region segmentation, represented by the Harvard-Oxford brain atlas (integrated into the Conn atlas). We presented this type of brain-region segmentation in the main text **??**, where we coloured the regions on the circle with their own cognitive domain. To determine these regions' cognitive domains, we assigned each region's an ICN membership according to the maximum voxel overlap of its spatial location with the ICN-BM20 network atlases (Figure S3) (Kozák et al., 2017).

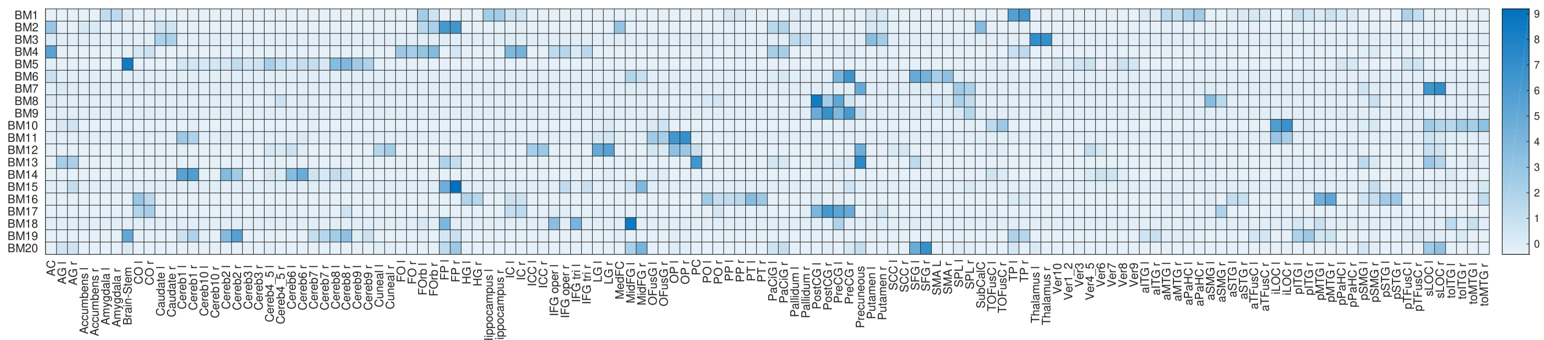

Figure S3. The correspondence between brain regions and ICNs. The brain regions were segmented with the Conn region atlas. Color bar indicates normalised (across BM atlases for each brain region) ICN involvement. The BM atlas having the highest level of correspondence (i.e., the biggest values in every column) with the region was considered the large-scale network that this region belongs to.

Correspondence of significant brain regions in the PPI analysis to ICNs

Using PPI we found that as cognitive demand increased, task-related FC (trFC) increased between the vPCu and IoN and between the dPCu and EoN. However, when the cognitive demand was low the trFC association was reversed (**??**). An additional hierarchical clustering analysis provided further evidence that the trFC between the d/vPCu and IoN/EoN were reversed by different levels of difficulty (Figure S4 in the Supplementary Materials).

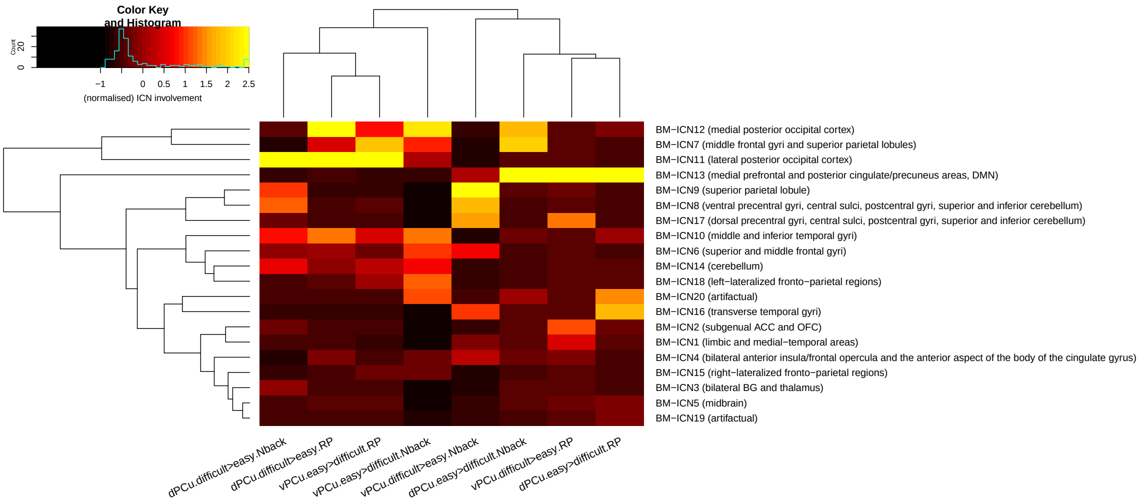

Figure S4. Hierarchical clustering of the PPI results showing the interplay between the trFC of the d/vPCu and internally/externally oriented networks. The brightness values in the heatmap represent normalised ICN spatial involvement (normalised across the 20 network domains per seed per condition per task). The distribution of ICN spatial involvement is shown in the top left corner. To visually identify patterns, the rows and columns of a heatmap are sorted by hierarchical clustering trees.

ICN spatial involvement and brain heatmaps of the v/dPCu's task-state FC (tsFC)

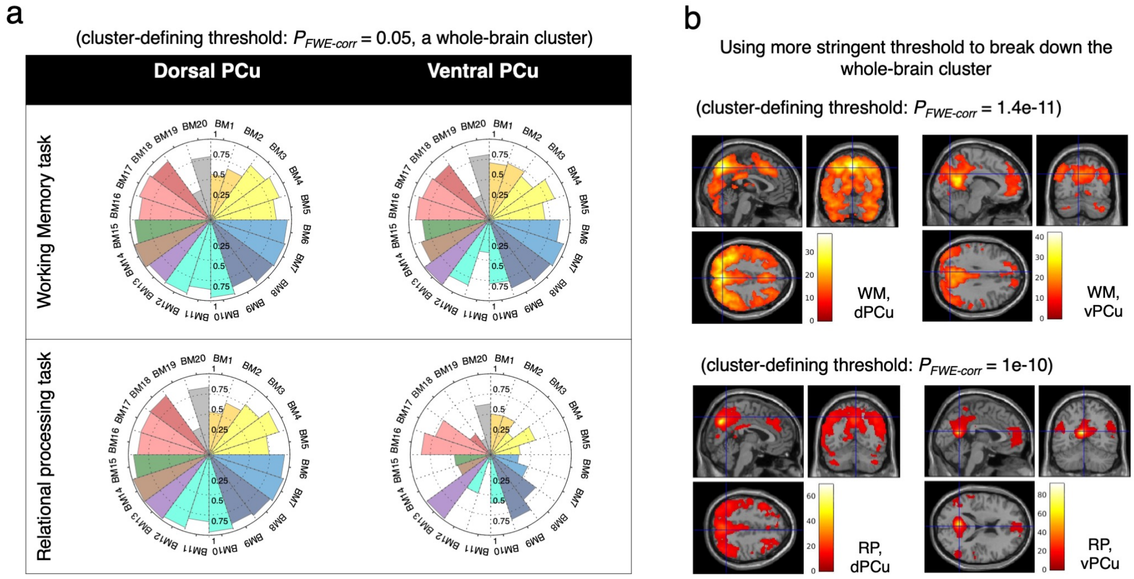

Figure S5. (a) ICN Spatial Involvement of the d/vPCu' FC during tasks. The dPCu is functionally coupled with brain regions of all domains while the vPCu's FC is more constrained to the DMN during tasks. (b) Brain heatmaps of the d/vPCu's FC using extremely high voxel-level cluster-defining threshold. Different stringent voxel-level thresholds were experimented in order to separate the cluster centered at the seed and its adjacent regions. Upon these extremely high thresholds, the vPCu's FC was found to be most strongly concentrated within the DMN; however, this pattern was not found in the dPCu's FC. Rather, the dPCu was invariably connected to the whole brain, especially to the cognitive control regions, such as the middle and dorsal lateral frontal regions, posterior parietal cortex, etc. The color bar indicates T scores.

The correspondence of the PPI results with the ICNs

We first conducted PPI analyses independently for the two tasks and we observed a common pattern of the trFC between the N-back and the RP tasks. We then focused on the common pattern by averaging the individual-level trFC between the two tasks, and we conducted another group inference based on the individual averaged beta values. The task-averaged trFC was presented in the main article, while the relevant results independently for the two tasks were presented here.

In order to establish the point that the v/dPCu' FC with the internally/externally oriented networks is modulated in reversed way by cognitive demand, we have used various ways of representing the PPI results. There are many different quantifiable ways to evaluate the ICN's involvement in/overlap with an existing whole-brain map result, but they are large consistent with each other.

Here we provided three ways of evaluating the ICN's involvement with the ICN_atlas toolbox: (1) the ICN Spatial Involvement (a measure reported in the main article), which calculates the voxel overlap between the thresholded and binarised ICN and T-score maps over the ICN volume (Figure S6; Equation (1)); (2) the ICN Relative Spatial Involvement, which calculates the number of voxel overlaps between a result map and a ICN but the denominator of the ratio is the total number of "overlapped" ICNs (Figure S7; Equation (2)); (3) the Spatial Overlap, defined by (Kim and Lee, 2012) (Figure S8; Equation (3)).

ICN$_i$ spatial involvement

$$I_i = \frac{|SPM_t \cap ICN_i|}{|ICN_i|} \tag{1}$$

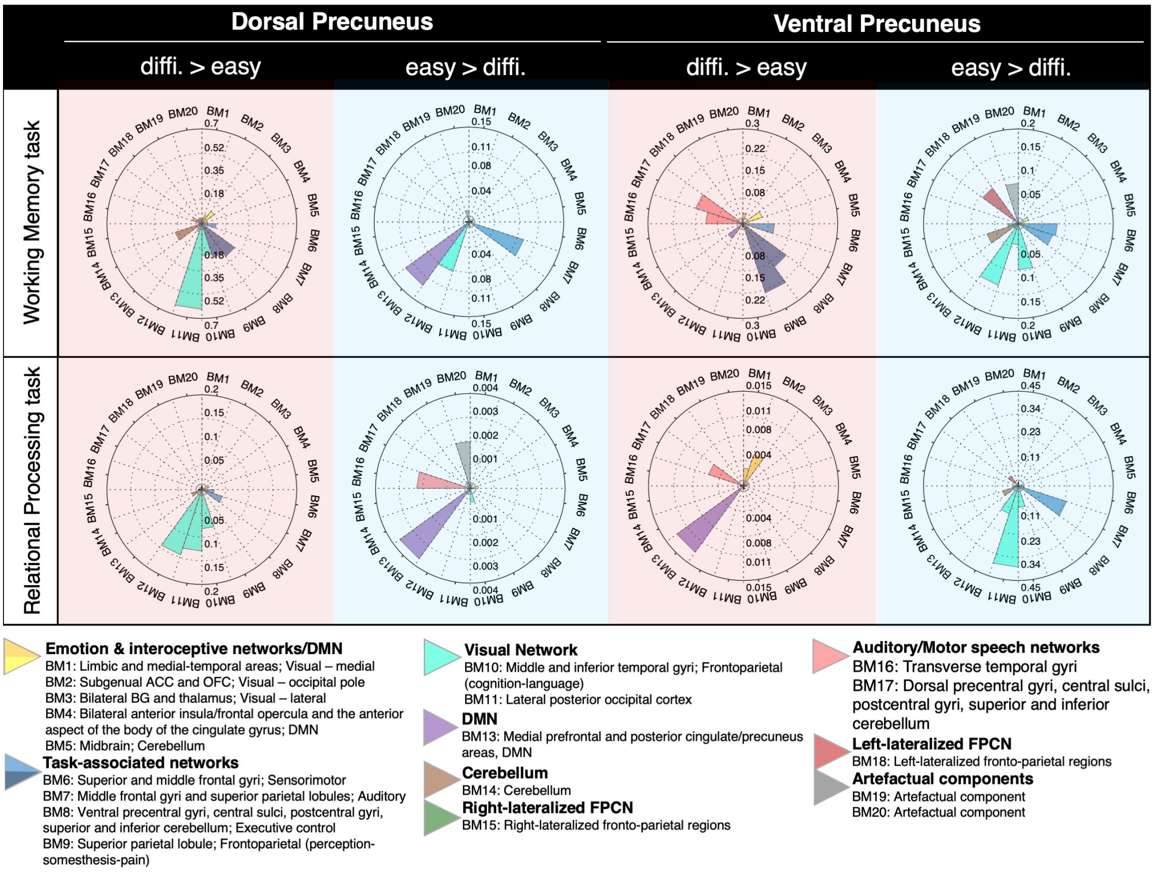

Figure S6. ICN spatial involvement of the PPI results. Examined regions are the significant clusters from the whole-brain PPI estimation (standard SPM approach), of which the FC with the seed (dorsal or ventral precuneus) was modulated by the task difficulty. The circular wedge plot provides a breakdown of the ICN correspondence with these significant regions.

ICN$_i$ relative spatial involvement

$$IR_i = \frac{|SPM_t \cap ICN_i|}{\sum_i |SPM_t \cap ICN_i|} \tag{2}$$

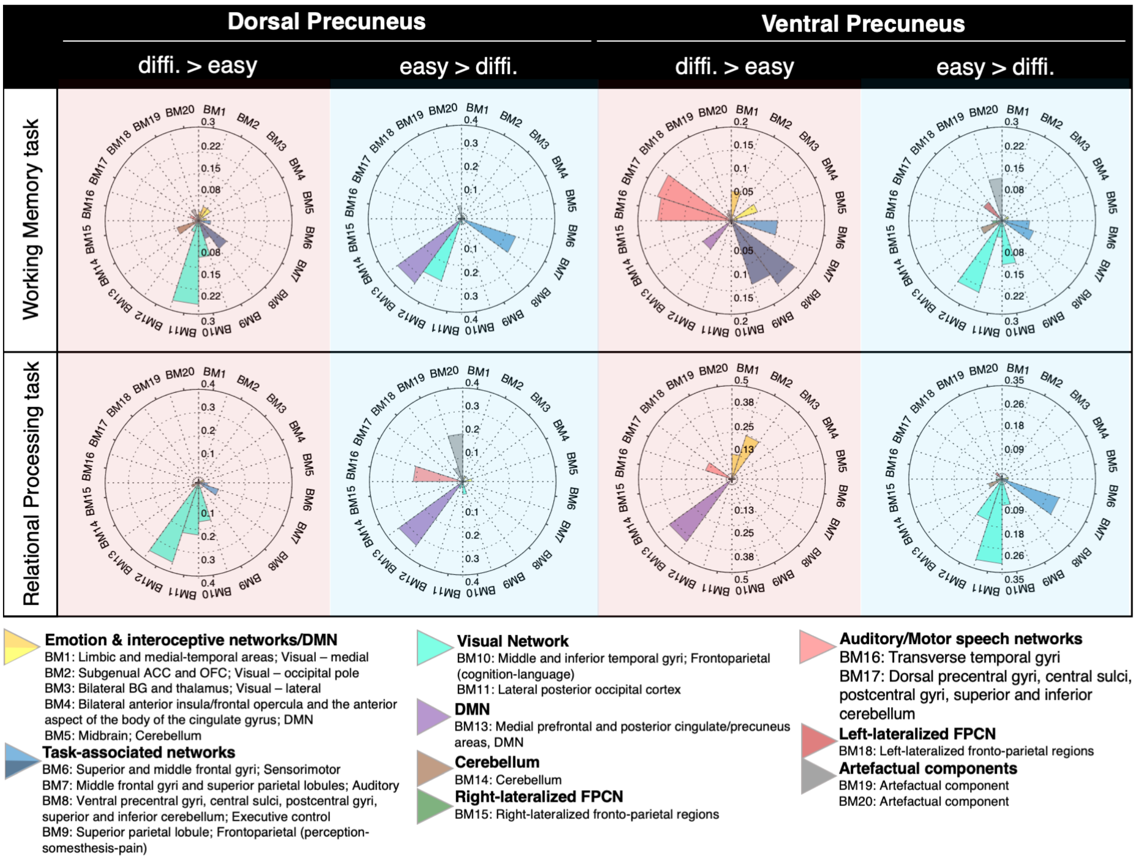

Figure S7. ICN relative spatial involvement of the PPI results. ICN spatial relative involvement of the PPI results. Examined regions are the significant clusters from the whole-brain PPI estimation (standard SPM approach), of which the FC with the seed (dorsal or ventral precuneus) was modulated by the task difficulty. The circular wedge plot provides a breakdown of the ICN correspondence with these significant regions.

ICN$_i$ spatial overlap

$$IR_i = \sqrt{\frac{(|SPM_t \cap ICN_i|)^2}{|SPM_t| \cdot |ICN_i|}} \tag{3}$$

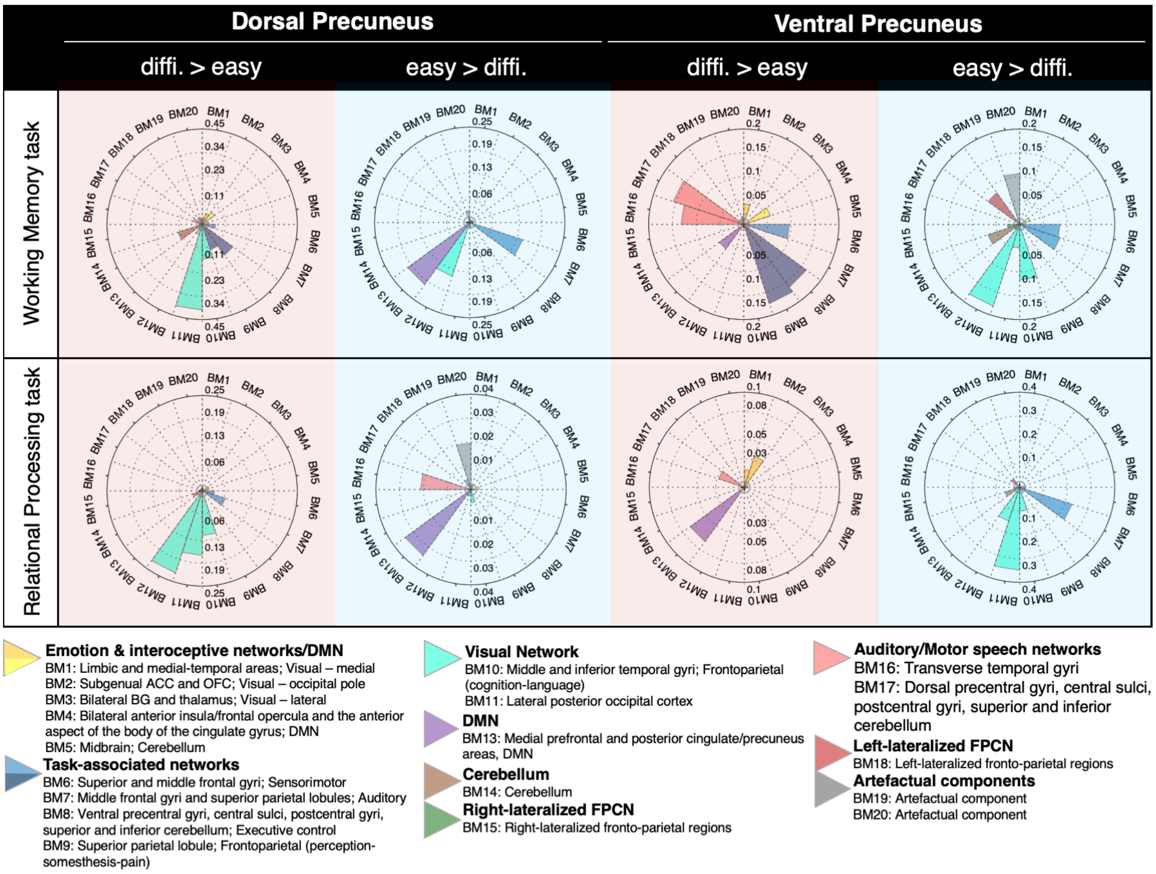

Figure S8. ICN spatial overlap of the PPI results. ICN spatial overlap of the PPI results. Examined regions are the significant clusters from the whole-brain PPI estimation (standard SPM approach), of which the FC with the seed (dorsal or ventral precuneus) was modulated by the task difficulty. The circular wedge plot provides a breakdown of the ICN correspondence with these significant regions.

SM References

Kim, Yong-Hwan and Jong-Hwan Lee. 2012. "Group Inference of Default-Mode Networks from Functional Magnetic Resonance Imaging Data: Comparison of Random- and Mixed-Effects Group Statistics." *International Journal of Imaging Systems and Technology* 22(2):121–131.

Kozák, Lajos R., Louis André van Graan, Umair J. Chaudhary, Ádám György Szabó and Louis Lemieux. 2017. "ICN_Atlas: Automated Description and Quantification of Functional MRI Activation Patterns in the Framework of Intrinsic Connectivity Networks." *Neuroimage* 163:319–341.